

METAMICT AND CHEMICALLY ALTERED VESUVIANITE

RAY K. EBY¹, JANUSZ JANECZEK² AND RODNEY C. EWING

Department of Geology, University of New Mexico, Albuquerque, New Mexico 87131, U.S.A.

T. SCOTT ERCIT

Mineral Sciences Section, Canadian Museum of Nature, Ottawa, Ontario K1P 6P4

LEE A. GROAT

Department of Geological Sciences, University of British Columbia, Vancouver, British Columbia V6T 2B4

BRYAN C. CHAKOUMAKOS

Solid State Division, Oak Ridge National Laboratory, P.O. Box 2008, Oak Ridge, Tennessee 37831-6056, U.S.A.

FRANK C. HAWTHORNE

Department of Geological Sciences, University of Manitoba, Winnipeg, Manitoba R3T 2N2

GEORGE R. ROSSMAN

Division of Geological Sciences, California Institute of Technology, Pasadena, California 91125, U.S.A.

ABSTRACT

Partly metamict vesuvianite samples from two localities were examined and compared. The unit cell of one is enlarged owing to volume expansion caused by the buildup of radiation damage. The other sample sustained enough damage to exclude accurate determination of unit-cell parameters. BSE imaging shows that both samples have undergone chemical alteration, and electron-microprobe data indicate that the alteration has resulted in a heterogeneous distribution of radionuclides on the micrometer scale. HRTEM and SAED analyses reveal a wide variation in the extent of alpha-recoil damage, which corresponds to the heterogeneous distribution of the radionuclides. The progressive stages of metamictization also are observed in detail with TEM. Partly metamict vesuvianite recrystallizes over the range 600–850°C, which is broader than the range found in other metamict silicates. Combined thermogravimetric analysis and isothermal annealing show that, upon heating (in N₂ or Ar), metamict vesuvianite begins to recrystallize at 600°C, and at 900°C decomposes into the multiphase assemblage grossular + gehlenite + wollastonite. Unpolarized IR spectra of both vesuvianite samples are similar and also resemble those of radiation-damaged zircon and titanite, suggesting that the major structural features of the aperiodic state are similar for complex ceramics of different composition.

Keywords: vesuvianite, metamict, radiation damage, alteration, transmission electron microscopy, back-scattered electron imaging, infrared spectroscopy, thermogravimetric analysis.

SOMMAIRE

Nous avons étudié et comparé des échantillons de vésuvianite partiellement métamictite provenant de deux endroits. La maille élémentaire dans un cas est agrandie par les effets du dommage structural dû à l'irradiation. L'autre échantillon a subi suffisamment de dommage pour rendre impossible la détermination des paramètres du réseau. Les images obtenues avec électrons rétrodiffusés montrent que dans les deux cas, la vésuvianite a subi une altération chimique. Les données à la microsonde électronique démontrent

¹ Present address: TopoMetrix, One Robertson Drive, Suite 18, Bedminster, New Jersey 07921, U.S.A.

² Present address: Department of Earth Sciences, Silesian University, Bedzinska 60, 41-200 Sosnowiec, Poland.

une distribution hétérogène des radionucléides à l'échelle micrométrique. Les analyses par microscopie électronique par transmission à haute résolution, avec diffraction des électrons sur domaines restreints, révèle une grande variation dans la portée du dommage dû au resac des nucléus par particules alpha, qui correspond à la distribution hétérogène des radionucléides. La progression de la métamictisation peut être documentée en détail par microscopie électronique par transmission. On peut recristalliser la vésuvianite partiellement métamictique en la chauffant entre 600 et 850°C, un intervalle plus grand que pour les autres silicates métamictiques. Une combinaison d'analyse thermogravimétrique et de traitement par recuit isothermal montre qu'en présence de N₂ ou Ar, il y a un début de recristallisation à 600°C, et qu'à 900°C, la vésuvianite se décompose en un assemblage multiphasé de grossulaire, gehlenite et wollastonite. Les spectres d'absorption infra-rouge non polarisés des deux échantillons sont semblables, et ressemblent à ceux de zircon et de titanite endommagés par irradiation. Ces résultats font penser que les éléments structuraux typiques de l'état aperiodique développé aux dépens de matériaux céramiques complexes de compositions différentes se ressemblent.

(Traduit par la Rédaction)

Mots-clés: vésuvianite, métamictique, dommage par irradiation, altération, microscopie électronique par transmission, images par électrons rétrodiffusés, spectroscopie d'absorption infra-rouge, analyse thermogravimétrique.

INTRODUCTION

Radiation damage resulting from alpha-decay (metamictization) is rare in vesuvianite, because U and Th are not usually present in appreciable amounts. The amount of U and Th found in partly metamict minerals is typically several hundred ppm, and fully metamict minerals may contain several thousand ppm of U and Th. Two samples of vesuvianite exhibiting metamict characteristics were examined using high-resolution transmission electron microscopy (HRTEM), selected-area electron diffraction (SAED), powder X-ray diffraction (XRD), electron-microprobe analysis (EMPA), back-scattered electron (BSE) imaging, thermogravimetric analysis (TGA) and infrared spectroscopy (IR). These samples of vesuvianite were previously characterized by Groat *et al.* (1992), and the same sample numbers are used here. Sample V53 is from the Seward Peninsula, Alaska, where it occurs as large (up to 1.5 cm) brown crystals in a highly radioactive nepheline syenite of mid-Cretaceous age (Himmelberg & Miller 1980, Miller & Bunker 1976). Sample V73 is a large (2 cm) black crystal with conchoidal fracture, from a skarn near Lake George, Colorado. The only other reported locality for metamict vesuvianite is an alkaline pegmatite in the Tuva district, in the former USSR. Samples from this locality were studied using thermal analysis methods (Kononova 1960). The vesuvianite from Tuva shows an exothermic peak and weight-loss over the range 650–750°C (corresponding to recrystallization), and then decomposes into garnet above 900°C.

Metamictization results from the alpha-decay process via the U/Th decay series. An alpha-event produces two particles: i) a 4.0–5.5 MeV alpha particle, which travels relatively far through the structure (~20 µm) and causes negligible amorphization by elastic collision, but produces significant ionization effects in the form of isolated point defects and associated structural strain; ii) a 75–90 keV alpha-recoil nucleus, which travels approximately 20 nm, and results in 1500–2000 atomic

displacements (*i.e.*, a collision cascade) and limited ionization-related effects. Alpha-recoil collision cascades result in localized aperiodic regions that have recently been observed with HRTEM in titanite (Lumpkin *et al.* 1991). For extensive reviews of radiation effects in minerals and ceramics, see Wang & Ewing (1992), White *et al.* (1989), Ewing *et al.* (1987), Clinard & Hobbs (1986) and Thompson (1981).

EXPERIMENTAL METHODS

Electron-microprobe analysis

Electron-microprobe analyses (EMPA) were carried out with a JEOL 733 instrument (at Ottawa); experimental details are given by Groat *et al.* (1992). The following standards were used: riebeckite (F), Na-bearing amphibole (Na), almandine (Mg, Al, Fe), diopside (Si), anhydrite (S), tugtupite (Cl), synthetic gehlenite (Ca), titanite (Ti), tephroite (Mn), LaPO₄ (La), CePO₄ (Ce), PrPO₄ (Pr), ThO₂ (Th) and UO₂ (U). The following elements were sought, but not detected: B, K, Cr, Zn, Sb, Nd, Sm, Pb and Bi. Back-scattered electron (BSE) imaging was done with the JEOL 733 electron microprobe and with a Nanolab 7 scanning electron-microscope (at UBC).

X-ray diffraction

Unit-cell dimensions were determined with a Nicolet R3m single-crystal diffractometer (at the University of Manitoba); experimental details are given by Groat *et al.* (1992). Powder XRD patterns of annealed sample V73 were acquired with CuKα radiation using SCINTAG diffractometers, one equipped with a monochromator and scintillation detector (at the University of New Mexico) and one equipped with an intrinsic Ge detector (at Oak Ridge National Laboratory). Owing to the small amount of material, sample mounts consisted of thin slurries on a zero-background quartz holder.

Transmission electron microscopy

Vesuvianite samples were prepared for TEM analysis using the crushed-grain method. Sample fragments were ground into 1–5 µm powder and dispersed in acetone onto holey-carbon Cu grids. One sample of V73 was also prepared by ion-milling, which permitted detailed analysis of *in situ* features. Specimens were examined with a JEOL 2000FX TEM operated at 200 keV, using standard axial illumination and phase-contrast imaging for high-resolution work and SAED. A preliminary examination of nonmetamict vesuvianite indicates that electron-beam radiation damage is easily avoided during high-resolution imaging, thereby justifying the use of HRTEM for the examination of amorphization features. All SAED patterns were focused on the objective aperture (aligned with the back focal plane) in order to provide a consistent representation of broadening of the diffraction maxima.

Annealing and thermogravimetric analysis

Annealing of TEM-analyzed samples was done in a sealed, inert, Ar atmosphere for 2 hours each, at 650, 700, 750, and 800°C with sample V73, and at 650°C with sample V53. Samples were crushed and encapsulated in gold envelopes for heating, thus preventing any reaction with the capsule walls. Annealing of XRD-analyzed samples was done using a Deltech programmable furnace. Isothermal annealing of sample V73 was done at 400, 600, 800, 900 and 1000°C, for 24 hours at each temperature, in flowing nitrogen. To further confirm the identity of the decomposition products of vesuvianite above 900°C, two highly crystalline reference samples, one (deep coffee brown) from a skarn in Phillips, Franklin County, Maine, and the other (yellow brown) from Lake Jaco, Chihuahua, Mexico, were heated at 1000°C in flowing Ar for 15 hours. The powdered samples rested on a platinum foil to prevent contamination and reaction with the substrate.

Thermogravimetric analyses (TGA) of sample V73 and the two reference samples were done at a heating rate of 10°C/min to 1000°C, in flowing argon, using a Perkin–Elmer TGS–2 system.

Infrared spectroscopy

High-resolution infrared spectra of single-crystal vesuvianite samples were recorded on a Nicolet model 60 SX Fourier-transform infrared spectrophotometer. Single crystals were sawn into slices, attached to glass slides with Crystalbond®, ground to 100 µm thick and polished on both sides. Spectra were taken through a 100-µm brass aperture that was positioned to avoid cracks and visible inclusions. The spectral contribution of the glass slide and Crystalbond were subsequently removed during spectral processing, and spectra for both samples were normalized to a thickness of 100 µm.

RESULTS AND DISCUSSION

Chemical compositions and BSE imaging

Results of chemical analyses of V53 and V73 are given in Table 1. Unit formulae were recalculated on the basis of 50 cations and were assigned to specific structural sites, as recommended by Groat *et al.* (1992).

Himmelberg & Miller (1980) reported that vesuvianite from the Seward Peninsula is optically zoned, with an isotropic (*i.e.*, metamict) core and anisotropic (*i.e.*, crystalline) rim. No optical or chemical zoning was observed in sample V53; however, BSE imaging of the chemically analyzed region (Fig. 1) shows three areas of varying contrast (*i.e.*, different average atomic number). Compositions V53–1 to V53–3 (Table 1) pertain to the light, medium and dark grey areas of Figure 1, respectively (each of these areas has a unique composition). The different compositions, combined with differing BSE contrast, suggest that chemical alteration has occurred. The medium grey zone contains no U, and less

TABLE 1. CHEMICAL COMPOSITION OF PARTLY METAMICT VESUVIANITE*

	V53-1	V53-2	V53-3	V73-1	V73-2	V73-3
SiO ₂ wt.%	34.01	34.73	39.08	34.96	34.96	34.07
Al ₂ O ₃	11.28	12.59	10.87	15.05	16.05	15.26
TiO ₂	2.52	2.79	3.28	1.28	0.82	0.95
MgO	1.80	1.85	1.31	2.21	1.98	1.70
MnO	0.11	0.10	0.00	0.66	0.41	0.34
FeO	7.93	6.69	7.55	4.98	4.43	4.11
CaO	30.03	31.33	16.63	35.26	34.96	30.35
Na ₂ O	0.30	0.36	0.16	0.00	0.00	0.18
La ₂ O ₃	1.37	0.87	1.34	0.00	0.00	0.00
Ce ₂ O ₃	2.58	1.78	2.23	0.00	0.00	0.00
Pr ₂ O ₃	0.23	0.24	0.28	0.00	0.00	0.00
Nd ₂ O ₃	0.88	0.46	0.79	0.00	0.00	0.00
ThO ₂	1.62	1.07	1.99	0.00	0.49	0.83
UO ₂	0.38	0.00	0.34	0.00	0.00	0.00
SO ₃	0.15	0.00	0.13	1.00	2.42	2.75
F	1.76	1.54	1.00	0.14	0.21	0.53
Cl	0.00	0.00	0.00	0.14	0.21	0.53
H ₂ O	1.71	1.94	-1.37	2.09	1.73	1.03
O=F,Cl	98.42	98.34	85.59	99.05	98.87	91.48
O=F,Cl	0.74	0.65	0.42	1.05	1.21	1.15
TOTAL	97.68	97.69	85.17	98.00	97.68	90.93
Si ⁴⁺	18.17	18.12	23.55	17.58	17.64	18.52
Al ³⁺	7.10	7.74	7.72	8.92	9.54	9.78
Ti ⁴⁺	1.01	1.09	1.48	0.48	0.35	0.59
Mg ²⁺	1.43	1.44	1.18	1.56	1.47	1.38
Mn ²⁺	0.06	0.04	0.00	0.28	0.19	0.16
Fe ²⁺	3.54	2.92	3.81	2.09	1.87	1.87
Ce ²⁺	17.19	17.51	10.74	18.99	18.90	17.88
Na ⁺	0.31	0.38	0.19	0.00	0.16	0.17
La ³⁺	0.27	0.17	0.30	0.00	0.00	0.00
Ce ³⁺	0.50	0.34	0.49	0.00	0.00	0.00
Pr ³⁺	0.04	0.05	0.06	0.00	0.00	0.00
Nd ³⁺	0.13	0.09	0.17	0.00	0.00	0.00
Th ⁴⁺	0.20	0.13	0.27	0.00	0.00	0.00
U ⁴⁺	0.04	0.00	0.05	0.00	0.06	0.06
Sr ⁺	0.06	0.00	0.06	0.00	0.00	0.00
F ⁻	2.67	2.54	1.91	3.85	4.39	4.21
Cl ⁻	0.00	0.00	0.00	0.12	0.18	0.49
OH ⁻	6.08	8.76	-5.51	7.00	5.81	3.74
ΣX	18.69	18.64	12.27	18.99	18.95	17.91
ΣY	13.14	13.24	14.18	13.43	13.41	13.57
ΣZ	18.17	18.12	23.55	17.58	17.64	18.52

*Vesuvianite analyses are normalized on 50 total cations. H₂O is calculated for charge balance.

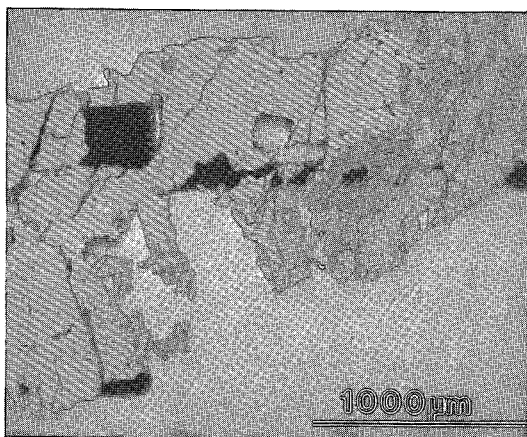


FIG. 1. Back-scattered electron image of V53. Chemical alteration is represented by areas of differing contrast (*i.e.*, different atomic mass); the light, medium and dark grey areas each have a different composition, corresponding to compositions V53-1, V53-2 and V53-3, respectively, in Table 1.

La, Ce and Nd, than the other areas. The darkest zone has a low oxide total (85.17%). Severe depletion of Ca is responsible for this low total, indicating that the dark region has sustained appreciable chemical alteration. Overall, sample V53 contains 3.35 – 4.84 wt.% of rare-earth elements, expressed as oxides (0.65 – 1.02 atoms per formula unit, apfu), 1.07 – 1.99 wt.% ThO₂ (0.13 – 0.27 apfu) and 0.0 – 0.36 wt.% UO₂ (0 – 0.05 apfu). Himmelberg & Miller (1980) found 0.72 – 2.70 wt.% ThO₂ and 0.39 – 0.84 wt.% UO₂ in a sample from the same locality. The discrepancy in U/Th contents between the values of this study and those of Himmelberg & Miller (1980) is not surprising, because chemical alteration can produce highly variable results. Nevertheless, these U/Th values are unusually high for vesuvianite. V53 also contains up to 0.36 wt.% Na₂O and 7.93 wt.% FeO; these values also are high.

BSE imaging and phase identification with energy-dispersion spectrometry (EDS) indicate that sample V73 is a polycrystalline aggregate of vesuvianite (Fig. 2), with minor inclusions of titanite, uraninite, quartz, calcite, apatite, chlorite, magnetite, barite and zircon. Textures seen in BSE and optically in thin section suggest that these minerals crystallized at the same time. As with sample V53, areas of differing BSE contrast show a correlation with their composition; however, the

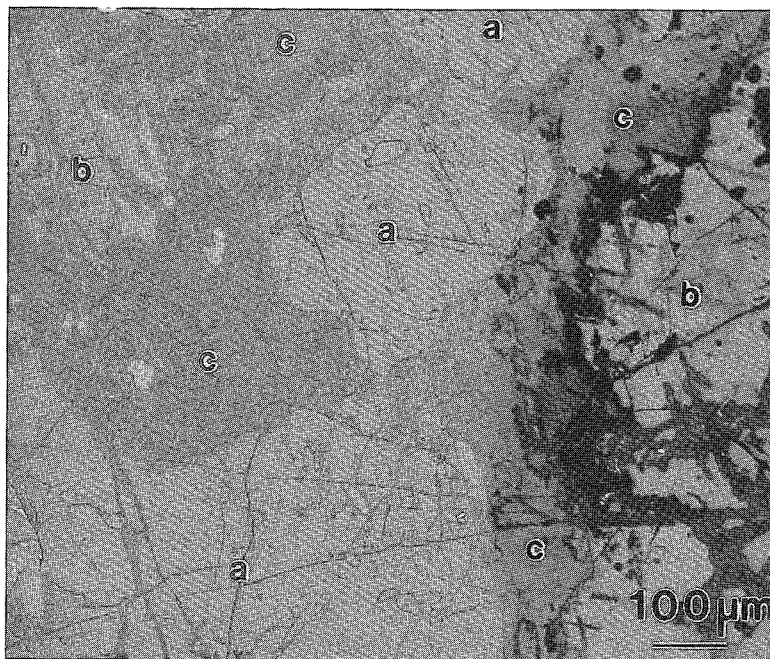


FIG. 2. Back-scattered electron image of V73. Chemical alteration is evident by the areas of different contrast. Regions labeled as *a*, *b*, and *c* correspond to U-poor, U-rich, and altered-rim U-rich compositions (V73-1, V73-2, V73-3, respectively, in Table 1).

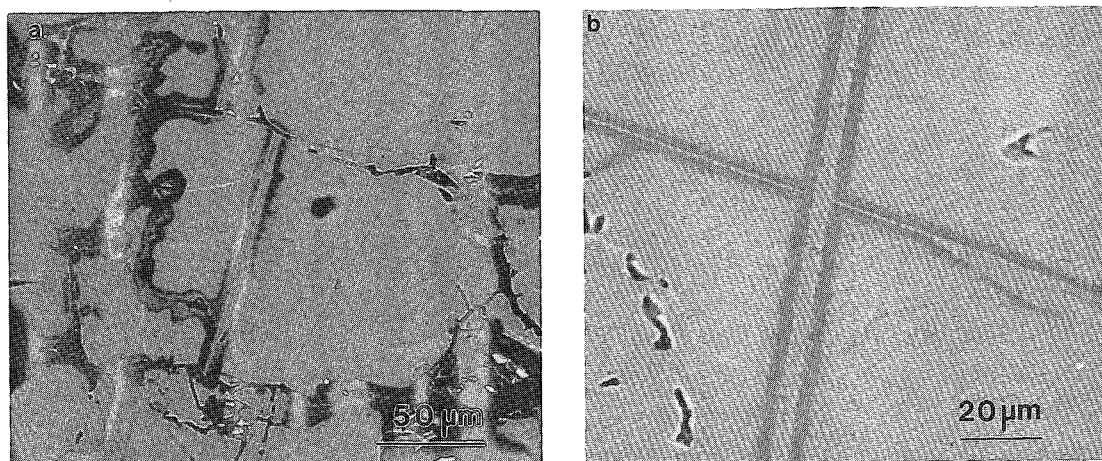


FIG. 3. Back-scattered electron image of V73. Sharply defined linear features have been filled in with titanite, uraninite, and vesuvianite. Their origin is uncertain. (a) A linear zone is offset by later fracturing. (b) Note the symmetrical pattern of alteration.

compositional differences and the degree of contrast are more subtle in V73. In general, those regions with a high U content are usually metamict and have an altered border. Chemical analyses (Table 1) were done on a U-poor region, a U-rich region, and the altered border of the U-rich region, respectively. Regions of dark contrast, labeled as (c) in Figure 2 and V73-3 in Table 1, are depleted in Ca. However, the U content of the altered border (V73-3) has not changed appreciably from that of the associated U-rich region (V73-2).

A series of subparallel, linear features in V73 were observed using BSE imaging. The linear features have been fractured and offset by later deformation (Fig. 3a), and appear to be leached by fluids because of the symmetrically banded pattern along their length (Fig. 3b). Within these features are titanite, vesuvianite and uraninite. Very straight edges suggest that they were once crystallographically controlled fractures. Considering that BSE is a surface imaging technique, the linear features must actually be planar in their true dimensions, because it is unlikely that we have cross-cut an entire set of one-dimensional features along the plane of observation. This rules out the possibility that they are fission tracks (also, they are much too long, >100 μm , and their subparallel orientations do not resemble the orientations of random tracks found in other track-bearing phases, *i.e.*, zircon or apatite). Chemical leaching of the "planar" features impedes their positive identification.

Unit-cell dimensions

The cell dimensions of V53 were determined: a 15.792(5) and c 11.993(8) Å. The a cell dimension is large for vesuvianite; most samples with a larger than 15.62 Å either contain boron or are partly metamict

(Groat *et al.* 1992). Cell dimensions for V73 were not obtained, because of the high degree of metamictization.

Transmission electron microscopy

Samples V53 and V73 are nonuniform in their degree of radiation damage from one crushed-grain fragment to the next. This is the result of small-scale variations in concentrations of radionuclides, as established with EMPA. Each crushed fragment has, within itself, a uniform amount of radiation damage, indicating that the size of similarly damaged regions is on the same order as that of the crushed grains used for TEM work (1–5 μm). A micrograph of undamaged vesuvianite from Brooks Mountains, Alaska, is shown in Figure 4 for comparison with subsequent micrographs of partly metamict vesuvianite.

A series of micrographs (Fig. 5) illustrate the full range of alpha-recoil damage observed in sample V53. Figure 5a shows a lattice image with fringes that are largely continuous, but that have mottled contrast and one localized amorphous region (indicated with an arrow). The SAED pattern gives no hint of radiation damage, because of the small volume of aperiodic material. The small amount of damage and lack of a diffuse electron-scattering halo in SAED are typical of a low alpha-decay dose of less than 0.05 dpa (displacements per atom) (less than 100 ppm). Low-dose damage has previously been examined in titanite with HRTEM (Eby & Ewing 1990). Calculation of dpa for both vesuvianite samples is not possible, as the age of the chemical alteration event(s) is unknown. An intermediate amount of damage is shown in Figure 5b. Alpha-recoil cascade regions are sufficiently numerous for overlap, resulting in the formation of continuous amor-

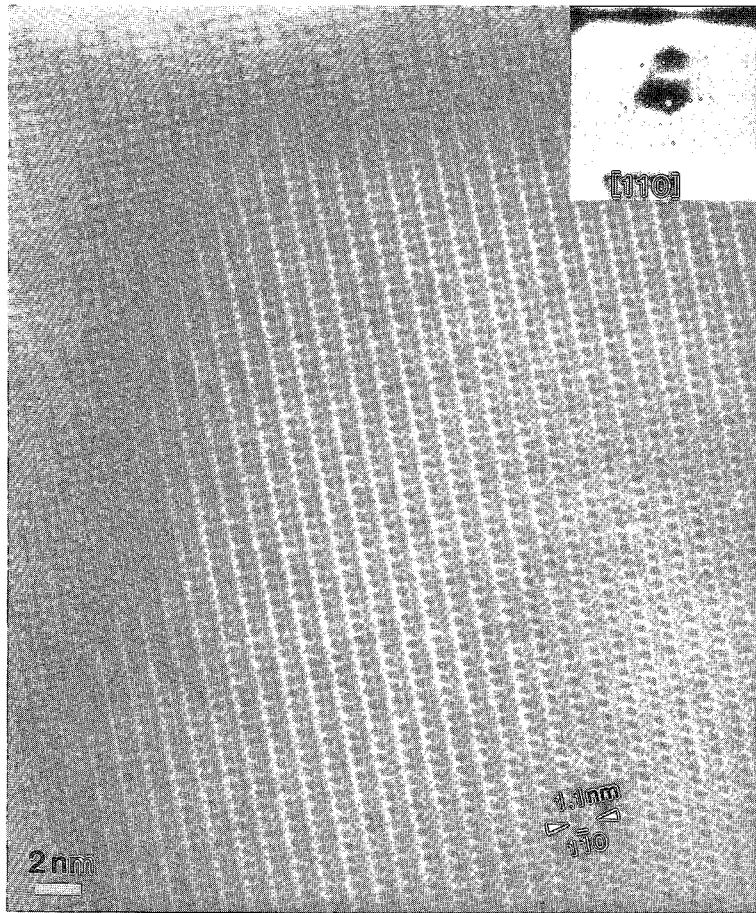


FIG. 4. A high-resolution electron micrograph of nonmetamict vesuvianite in $[110]$ zone-axis orientation.

phous regions which separate large, isolated regions of crystalline material. A diffuse electron-scattering halo is visible with SAED. The diffraction maxima are broadened and have unequal intensities relative to those in Figure 5a. The appearance of a diffuse halo coincides with the onset of discontinuity in the lattice fringes, both of which signify the beginning of overlap between amorphous regions (adjacent amorphous regions expand and coalesce). This observation is consistent with an earlier study in which $\text{Ga}_2\text{Ti}_2\text{O}_7$ and $\text{CaZrTi}_2\text{O}_7$ were doped with Cm (Weber *et al.* 1986). The coalescence of amorphous regions in these oxide phases coincides with the appearance of a diffuse halo in SAED. In the advanced state of radiation damage (Fig. 5c), the small crystalline regions that remain are surrounded by an amorphous matrix. Lattice fringes are barely visible because of the large amount of image interference from the amorphous material. The diffuse halo is stronger than

in Figure 5b, owing to the volumetric dominance of amorphous material. The single-crystal component of the SAED pattern has missing diffraction maxima (not due to extinction by symmetry), and relative intensities of the maxima vary considerably. The fully metamict state is shown in Figure 5d. No lattice fringes are visible in the phase contrast image, and no diffraction maxima are observed by SAED. Minute amounts of remaining crystalline matter may still exist, but are difficult to detect in SAED, since the strong intensity of the electron-scattering halo obscures the visibility of any weak diffraction-maxima that may be present.

A progressive sequence of increasing radiation damage in sample V73 is shown in a series of SAED patterns (Fig. 6). Figure 6a has sharp diffraction maxima and no halo, indicative of little or no alpha-decay damage. Figure 6b shows a single-crystal pattern with a superimposed weak halo. The state of damage is intermediate.

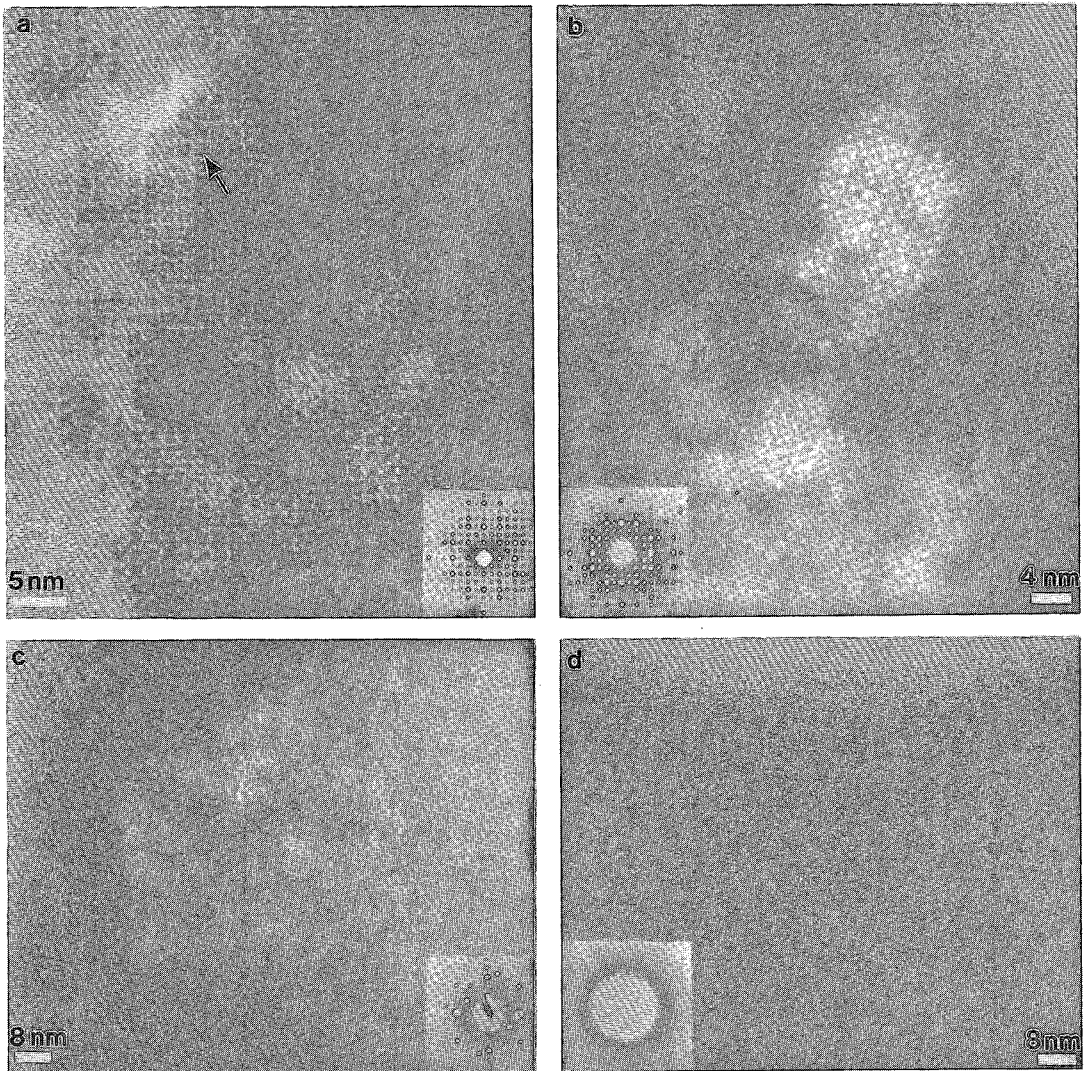


FIG. 5. A series of electron micrographs, each of a different crushed grain of sample V53. (a) A low amount of alpha-recoil damage; SAED is a [001] zone-axis pattern (ZAP). (b) A moderate amount of alpha-recoil damage; [001] ZAP. (c) An advanced state of alpha-decay damage. (d) The fully metamict state.

An advanced state of alpha-recoil damage is shown in Figure 6c, in which only a few diffraction-maxima remain and an intense halo is present. The grain examined in Figure 6d is a mixture of polycrystalline, randomly oriented grains (producing the diffraction rings) and amorphous material (producing the halo). The diffraction rings were indexed and match the d -values of vesuvianite. The polycrystalline state may be due to several causes; for example, i) high alpha-decay doses lead to subgrain formation, as observed in ion-irradiated neptunite (Eby *et al.* 1991) and naturally metamict

gadolinite (Janeczek & Eby 1991); ii) the material was initially polycrystalline and has since sustained radiation damage. Either case would result in the superposition of a halo onto a diffraction-ring pattern.

A further example of the heterogeneously distributed alpha-decay damage is shown by *in situ* observation of adjacent regions that have variable damage within an ion-milled single crystal (Fig. 7). Two regions of vesuvianite, marked with arrows (Fig. 7a), are separated by another silicate phase (confirmed by EDS analysis). At higher magnification, these two regions clearly

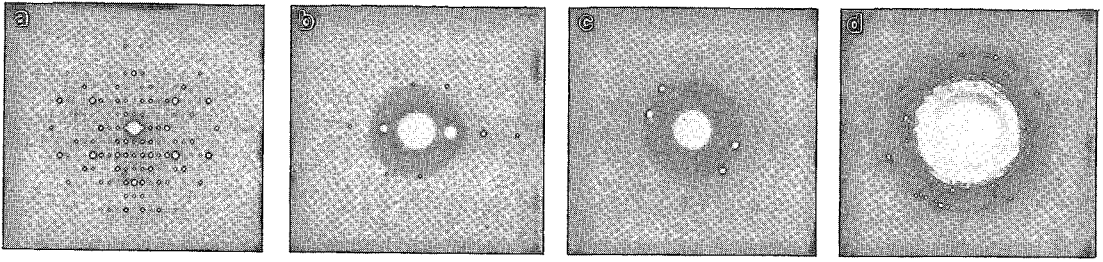


FIG. 6. A series of SAED of V73, with varying amounts of metamictization. (a) [011] ZAP of seemingly undamaged material. (b) An intermediate amount of alpha-recoil damage. (c) An advanced state of alpha-decay damage. (d) A polycrystalline grain with a significant amount of damage as well (note the halo). Ring d -values can be indexed as belonging to vesuvianite.

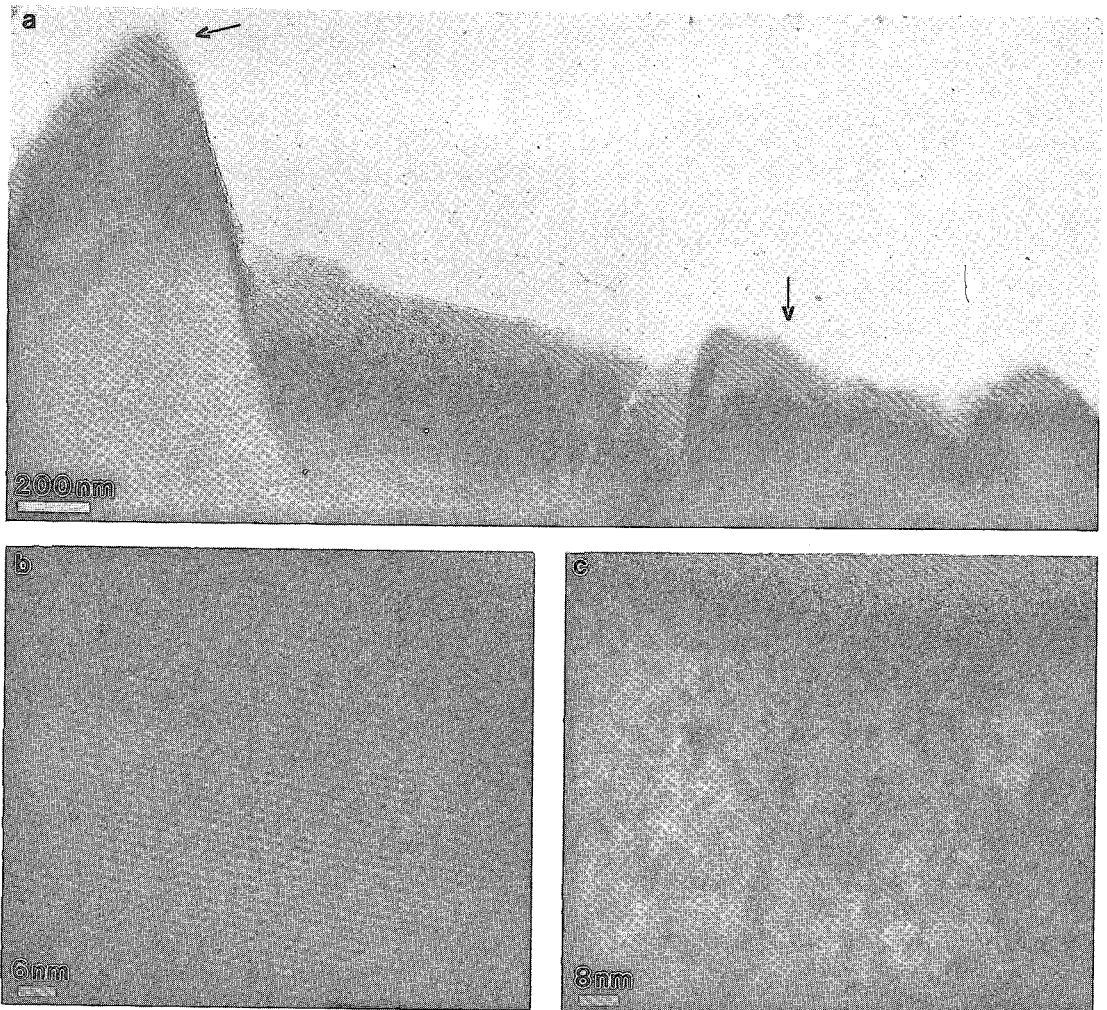


FIG. 7. (a) Electron micrograph of an ion-milled single crystal of V73 in [011] orientation. (b) A lattice image of the area in (a) near the left arrow. (c) A lattice image of the area in (a) near the right arrow. Note the difference in radiation damage between (b) and (c).

exhibit different degrees of radiation damage; the area in Figure 7b is undamaged and shows clean, unmottled lattice fringes; the area in Figure 7c has mottled, partly discontinuous lattice fringes with coalesced amorphous areas.

Annealing

XRD analyses of V73, following each heating interval of 200°C (in flowing nitrogen), indicate that recrystallization begins at approximately 600°C (Fig. 8). A few of the smaller diffraction-peaks are more intense. This minor increase in crystallinity coincides with an increase

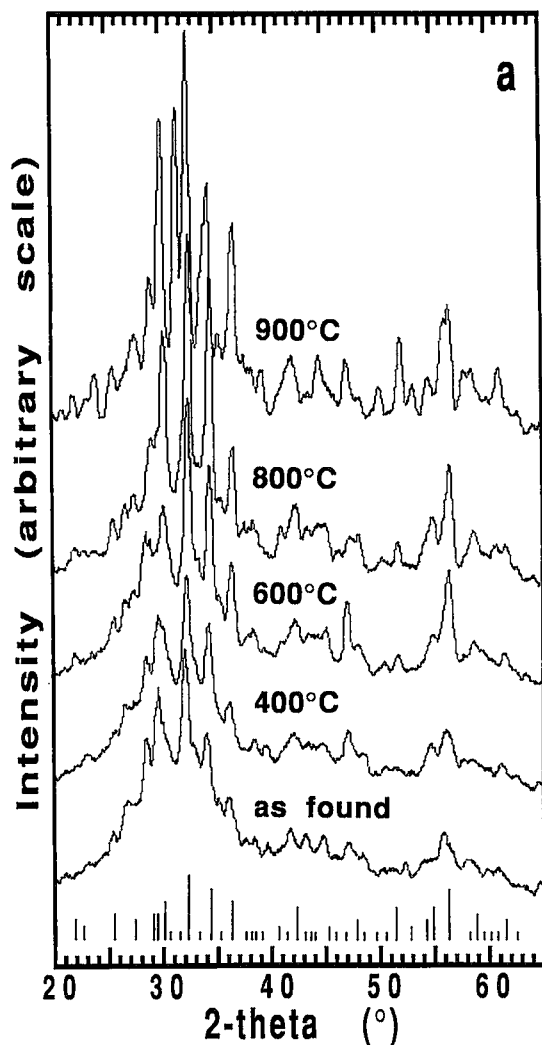


FIG. 8a. Powder XRD pattern (CuK α radiation) of sample V73 as found and annealed in nitrogen (24 hours each) at 400°, 600°, 800° and 900°C. The stick pattern at the bottom shows the peak positions and relative intensities typical of crystalline vesuvianite.

in the rate of weight loss in the TGA analysis, at approximately 600°C (Fig. 9). After heating V53 to 650°C, and V73 to 650°C and 700°C (in argon), TEM analysis shows no evidence of recrystallization. Figure 10a shows that many amorphous regions are still present in V73. Apparently, TEM is not sensitive to the onset of recrystallization, which most likely involves a subtle increase in the long-range periodicity of the structure as a result of annealing the isolated point-defects within less damaged regions. A two-stage (or more) sequence of recrystallization is thus likely. These observations and interpretations are consistent with similar work on allanite by Janeczek & Eby (1993).

At 800°C, XRD patterns indicate a significant improvement in the crystallinity of V73. Background intensity has decreased, and resolution of diffraction peaks has increased. The TGA curve (Fig. 9) flattens somewhat between 830°C and 900°C. Observation with TEM, after annealing to 750 and 800°C, indicates that much of the alpha-recoil damage has been annealed (there is no observable difference in recrystallization features between these two temperatures). Lattice fringes are continuous, but some grains still display mottled contrast between fringes. The variation in the state of repair between different grains presumably exists because the more damaged areas require a higher activation energy for recrystallization. Grains with little damage do not require the nucleation of newly crystalline material, and their localized amorphous regions can regrow epitactically at 800°C. The requirement of a higher temperature of annealing for more damaged material has been proposed for another silicate, titanite (Hawthorne *et al.* 1991). The amorphous material that remains in the more highly damaged areas implies that another thermal stage is necessary for full restoration of the structure.

Another feature appears at 750 and 800°C. Recrystallization is not yet complete, and heating of the material with the electron beam results in damage to some of the grains. Figure 10b shows the effects of beam damage, and should not be mistaken for natural radiation damage, most of which has been annealed. The beam-damaged grains were also observed to vibrate intensely. Grain vibration was also observed during annealing studies of titanite and gadolinite (Eby & Ewing 1990, Janeczek & Eby 1991), but was not previously reported.

For metamict vesuvianite, three stages of weight loss can be identified in the TGA curve (Fig. 9). Initially, the sample gradually dehydrates over the temperature range 150–600°C, losing 1 wt.%. Then, the rate of weight loss increases over the interval 600–850°C, in which the sample loses an additional 2 wt.%. Beyond 900°C, the rate of weight loss increases again (an additional 1 wt.%), and continues until the final measured temperature. Further explanation of the stages in weight loss can be made based on the XRD patterns of isothermally annealed samples, the differential thermal analysis (DTA) data of Kononova (1960), and the TGA data of

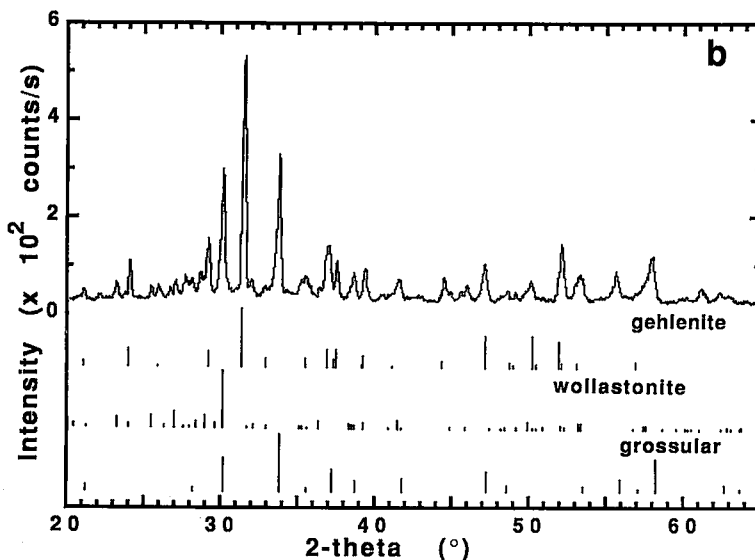


FIG 8b. Powder XRD pattern (CuK α radiation) of sample V73 decomposed at 1000°C (24 hours in nitrogen), with the major products of decomposition shown by stick patterns.

crystalline vesuvianite. Metamict vesuvianite begins to recrystallize at 600°C (in N₂ or Ar). At 900°C and above, the recrystallized vesuvianite decomposes. This is consistent with the DTA data, which show a broad exotherm between 600 and 800°C and an additional exotherm beginning at 870°C. The product of decomposition is a multiphase assemblage containing predominantly gros-

sular, gehlenite and wollastonite. The decomposition phases are not unique to the peculiar chemistry of the metamict vesuvianite, as two crystals of highly crystalline vesuvianite from other localities produce the same products. A nearly balanced reaction converts vesuvianite into 2 grossular + gehlenite + 2 wollastonite. According to the TGA curves of the two highly crystal-

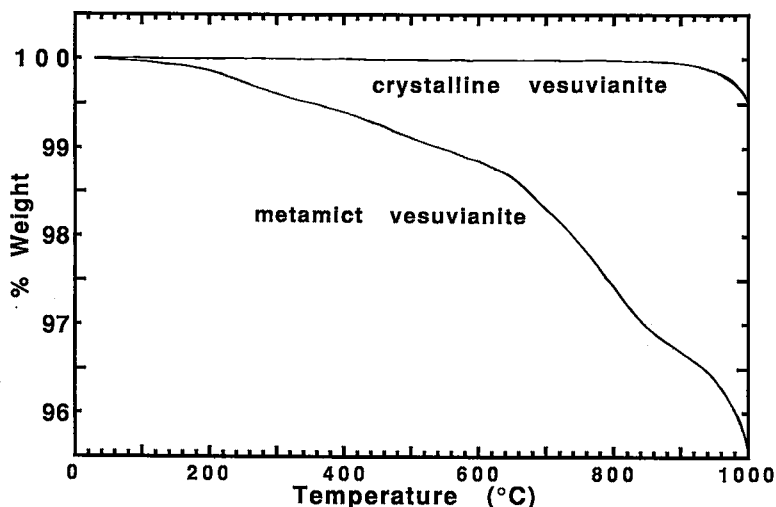


FIG. 9. Thermogravimetric analysis curves for V73 and a sample of crystalline vesuvianite from Phillips, Maine, heated at 10°C/min in flowing argon to 1000°C.

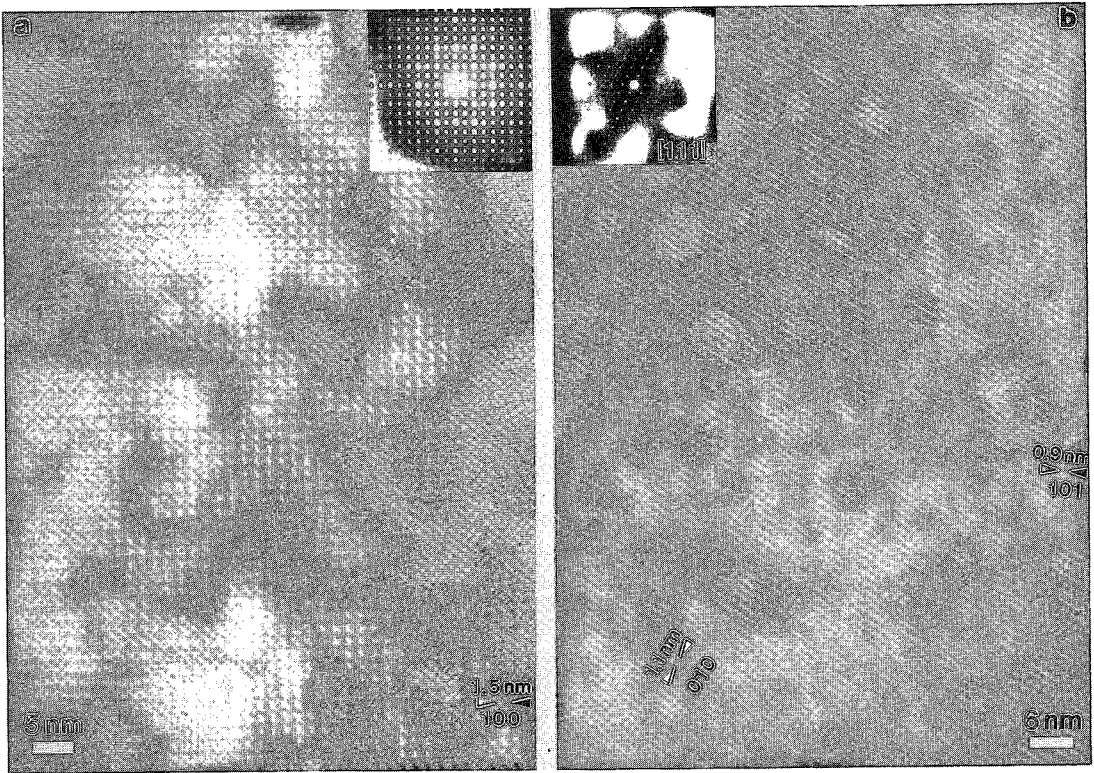


FIG. 10. (a) Electron micrograph of V73 heated to 650°C and corresponding [001] ZAP. Note that the alpha-recoil damage has not been removed. (b) Electron micrograph of V73 heated to 775°C and corresponding [111] ZAP. The numerous circular features are not results of natural radiation damage, but instead are due to damage caused by the electron beam.

line samples, the reaction probably evolves (OH), beginning at 900°C (Fig. 9).

Infrared spectroscopy

The infrared spectra of fully crystalline samples of vesuvianite are typically rich in detail within the principal OH-stretching region of 3800–2500 cm (Groat *et al.*, in prep.). In contrast, none of this detail remains in the spectra of the partly metamict vesuvianite. Spectra of samples V53 and V73 (Fig. 11) show a sharp increase in absorption at 3700 cm⁻¹, which reaches a maximum near 3475 cm⁻¹ and gradually decreases on the low-energy side down to 2500 cm⁻¹. This type of absorption also is observed in metamict zircon (Aines & Rossman 1986) and titanite (Hawthorne *et al.* 1991). However, the corresponding spectra of nonmetamict vesuvianite, titanite and zircon are quite different from one another, owing to the major structural differences between these

minerals. Thus, the similarity in the spectra of metamict minerals suggests that the distribution of major structural features of the aperiodic state (as probed by the strength of the O–H bond and its corresponding range of nearest neighbors) is similar, even for materials with different bulk-composition.

Furthermore, the individual bands are strongly anisotropic, indicating preferred crystallographic orientation of the individual OH environments.

The integrated intensity (Paterson 1982) of the primary OH band at 3475 cm⁻¹ indicates that sample V53 contains hydrous components (OH and H₂O) equivalent to 2.0 wt% H₂O, in reasonable agreement with the estimated water contents of Table 1. The intensity of the H₂O combination mode (stretch + bend) at 5200 cm⁻¹ indicates that only about 5% of the total water is in molecular form as H₂O. The remainder is present as OH. The dominance of OH was also observed in metamict zircon (Woodhead *et al.* 1991).

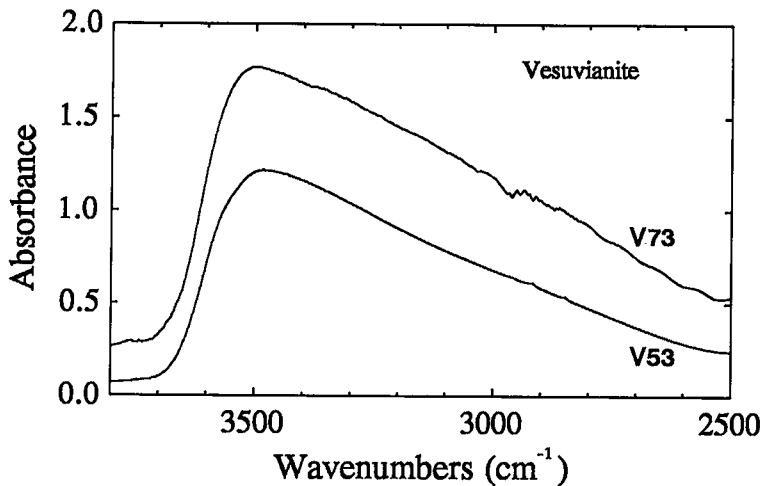


Fig. 11. Single-crystal infrared spectra of V53 and V73 in the principal OH-stretching region. Both spectra show the low-energy tailing absorption common in metamict minerals.

CONCLUSIONS

TEM analyses indicate that alpha-decay can leave vesuvianite intact, or make it partly metamict, or fully metamict, all within localized regions of the same sample. The variable concentrations of radionuclides that accompany the micrometer-scale zones of chemical alteration (ascertained by BSE imaging and EMPA) are responsible for the different extents of alpha-recoil damage observed in both samples of the vesuvianite. The relative differences in radiation damage were classified by observing: i) the variation of discontinuity in the lattice fringes; ii) the proportion of aperiodic area to lattice fringe area; iii) the intensity of the diffuse electron-scattering halo relative to the intensity of diffraction maxima.

Localized concentrations of alpha-recoil damage indicate that U and Th are not uniformly distributed throughout the specimens. The presence of uraninite in V73 indicates an abundance of U available for producing metamictization. Whether or not U was present in vesuvianite before alteration is unknown. A conservative estimate of the U/Th contents that are necessary to produce the observed variations in the metamict state can be calculated. First, assume that 0.1 dpa represents the lowest amount of alpha-recoil damage that can be observed, and that at least 1.0 dpa is required for the fully amorphous state. Such a variation in dpa requires a variation by one order of magnitude in U and Th concentrations. EMPA analyses of the two samples of vesuvianite show such a range, from less than 0.1 wt.% (*i.e.*, below detection limits) to 2.33 wt.% U and Th. Therefore, chemical alteration can have a profound effect on distribution of radionuclides and subsequent

alpha-recoil damage in minerals. Any attempt to calculate dpa in altered materials is futile unless the timing of the alteration event(s) is fully understood, because alteration also disturbs the structural state.

Alpha-decay damage in vesuvianite is annealed in at least two different stages. The proposed stages are: i) 600–750°C, the repair of point defects in partly metamict regions, which slightly improves the long-range periodicity (detected by XRD and TGA, but not TEM); ii) 750–800°C, the full repair of alpha-decay damage in partly metamict areas (detected by XRD and TEM, but not distinguished from the first stage by TGA); iii) above 850°C, material that was highly metamict is not recrystallized, but instead, vesuvianite decomposes into a multiphase assemblage of grossular, gehlenite, and wollastonite. The high structural and compositional complexity of vesuvianite, relative to most other minerals, may account for its high and broad thermal range of recrystallization as compared to the temperature ranges of other silicates, such as allanite and gadolinite, at 600–700°C (Janeczek & Eby 1991), REE-bearing epidote, at 600°C (Proshchenko *et al.* 1987), and titanite, at 400–600°C (Eby & Ewing 1990). Although temperature ranges for the recrystallization of metamict minerals show some variation, the structural features of the aperiodic state appear to be similar, at least as they pertain to the details of OH stretching.

ACKNOWLEDGEMENTS

Sample V73 was collected by a prospector, the late Bob Beal, who then brought the sample to Jack A. Adams, formerly of the U.S. Geological Survey, for identification. By XRD of the as-found and heated

sample, Adams identified the sample as metamict vesuvianite and later donated it to the Department of Geology, UNM. Roger Aines provided us with assistance in preliminary IR measurements of sample V53. Useful comments and suggestions were provided by Joe Blatz and Fred Shmuck, who reviewed the manuscript. NSERC of Canada provided assistance in the form of fellowships to RKE, operating grants to FCH and LAG, and an infrastructure grant to FCH. This work was also supported by Basic Energy Sciences of DOE, grant #DE-FGO4-84ER45099 to RCE. TEM was done in the Electron Microbeam Analysis Facility of the Department of Geology, UNM, supported in part by NSF, NASA, BES and the state of New Mexico. Research done at ORNL was supported by the Division of Materials Sciences, DOE contract #DE-AC05-84OR21400 with Martin Marietta Energy Systems, and at Caltech by NSF grant #EAR-8916064.

REFERENCES

- AINES, R.D. & ROSSMAN, G.R. (1986): Relationship between radiation damage and trace water in zircon, quartz and topaz. *Am. Mineral.* **71**, 1186-1193.
- CLINARD, F.W. & HOBBS, L.W. (1986): Radiation effects in non-metals. In *Physics of Radiation Effects in Crystals* (R.A. Johnston & A.N. Orlov, eds.). Elsevier, New York (387-471).
- EBY, R.K. & EWING, R.C. (1990): Annealing of alpha-recoil damage in natural titanite, CaTiSiO_5 . In *High Resolution Electron Microscopy of Defects in Materials* (U. Dahmen, R. Sinclair & D.J. Smith, eds.). *Mater. Res. Soc. Symp. Proc.* **183**, 297-300.
- _____, WANG, L.M., ARNOLD, G.W. & EWING, R.C. (1991): Ion-irradiation study of the "exotic" mineral neptunite: $\text{LiNa}_2\text{K}(\text{Fe}, \text{Mg}, \text{Mn})_2\text{Ti}_2\text{Si}_8\text{O}_{24}$. In *Surface Chemistry and Beam-Solid Interactions* (H.A. Atwater, F.A. Houle & D.H. Lowndes, eds.). *Mater. Res. Soc. Symp. Proc.* **201**, 283-286.
- EWING, R.C., CHAKOUMAKOS, B.C., LUMPKIN, G.R. & MURAKAMI, T. (1987): The metamict state. *Mater. Res. Soc. Bull.* **12**, 58-66.
- GROAT, L.A., HAWTHORNE, F.C. & ERCIT, T.S. (1992): The chemistry of vesuvianite. *Can. Mineral.* **30**, 19-48.
- HAWTHORNE, F.C., GROAT, L.A., RAUDSEPP, M., BALL, N.A., MITSUYOSHI, K., SPIKE, F., GABA, R., HALDEN, N.M., LUMPKIN, G.R., EWING, R.C., GREGOR, R.B., LYTLE, F.W., ERCIT, T.S., ROSSMAN, G.R., WICKS, F.J., RAMIK, R.A., SHERRIFF, B.L., FLEET, M.L. & MCCAMMON, C. (1991): Alpha-decay damage in titanite. *Am. Mineral.* **76**, 370-376.
- HIMMELBERG, G.R. & MILLER, T.P. (1980): Uranium- and thorium-rich vesuvianite from the Seward Peninsula, Alaska. *Am. Mineral.* **65**, 1020-1025.
- JANECZEK, J. & EBY, R.K. (1991): Annealing of the radiation damage in gadolinite. *Trans. Am. Geophys. Union* **72**, 554 (abstr.).
- _____, & _____ (1993): Annealing of radiation damage in allanite and gadolinite. *Phys. Chem. Minerals* **19**, 343-356.
- KONONOVA, V.A. (1960): On a metamict variety of vesuvianite from an alkaline pegmatite in southwest Tuva. *Dokl. Acad. Sci. USSR, Earth-Sci. Sect.* **130**, 129-132.
- LUMPKIN, G.R., EBY, R.K. & EWING, R.C. (1991): Alpha-recoil damage in titanite (CaTiSiO_5): direct observation and annealing study using high-resolution transmission electron microscopy. *J. Mater. Res.* **6**, 560-564.
- MILLER, T.P. & BUNKER, C.M. (1976): A reconnaissance study of the uranium and thorium contents of plutonic rocks of the southeastern Seward Peninsula, Alaska. *J. Res. U.S. Geol. Surv.* **4**, 367-377.
- PATERSON, M. (1982): The determination of hydroxyl by infrared absorption in quartz, silicate glasses, and similar materials. *Bull. Minéral.* **105**, 20-29.
- PROSHCHENKO, E.G., POLEZHAEV, M. & KHALEZOVA, E.B. (1987): Recrystallization characteristics of rare earth-containing epidotes. *Mineral. Zh.* **9**(4), 41-52 (in Russ.).
- THOMPSON, D.A. (1981): High density cascade effects. *Radiation Effects* **56**, 105-150.
- WANG, LU-MIN & EWING, R.C. (1992): Ion-beam-induced amorphization of complex materials - minerals. *Mater. Res. Soc. Bull.* **XVII/5**, 38-44.
- WEBER, W.J., WALD, J.W. & MATZKE, H. (1986): Effects of self-radiation damage in Cm-doped $\text{Gd}_2\text{Ti}_2\text{O}_7$ and $\text{CaZrTi}_2\text{O}_7$. *J. Nucl. Mater.* **138**, 196-209.
- WHITE, C.W., MCHARGUE, C.J., SKLAD, P.S., BOATNER, L.A. & FARLOW, G.C. (1989): Ion implantation and annealing of crystalline oxides. *Mater. Sci. Rep.* **4**, 41-146.
- WOODHEAD, J.A., ROSSMAN, G.R. & THOMAS, A.P. (1991): Hydrous species in zircon. *Am. Mineral.* **76**, 1533-1546.

Received March 23, 1992, revised manuscript accepted September 2, 1992.